



**HAL**  
open science

## Crystal Structure of the Complex mAb 17.2 and the C-Terminal Region of *Trypanosoma cruzi* P2 $\beta$ Protein: Implications in Cross-Reactivity

Juan Carlos Pizarro, Ginette Boulot, Graham A Bentley, Karina A Gómez, Johan Hoebeke, Mireille Hontebeyrie, Mariano J Levin, Cristian R Smulski

► **To cite this version:**

Juan Carlos Pizarro, Ginette Boulot, Graham A Bentley, Karina A Gómez, Johan Hoebeke, et al.. Crystal Structure of the Complex mAb 17.2 and the C-Terminal Region of *Trypanosoma cruzi* P2 $\beta$  Protein: Implications in Cross-Reactivity. PLoS Neglected Tropical Diseases, 2011, 5 (11), pp.e1375. 10.1371/journal.pntd.0001375 . hal-00643550

**HAL Id: hal-00643550**

**<https://hal.science/hal-00643550>**

Submitted on 2 Oct 2012

**HAL** is a multi-disciplinary open access archive for the deposit and dissemination of scientific research documents, whether they are published or not. The documents may come from teaching and research institutions in France or abroad, or from public or private research centers.

L'archive ouverte pluridisciplinaire **HAL**, est destinée au dépôt et à la diffusion de documents scientifiques de niveau recherche, publiés ou non, émanant des établissements d'enseignement et de recherche français ou étrangers, des laboratoires publics ou privés.

# Crystal Structure of the Complex mAb 17.2 and the C-Terminal Region of *Trypanosoma cruzi* P2 $\beta$ Protein: Implications in Cross-Reactivity

Juan Carlos Pizarro<sup>1,2\*</sup>, Ginette Boulot<sup>1,2</sup>, Graham A. Bentley<sup>1,2</sup>, Karina A. Gómez<sup>3</sup>, Johan Hoebeke<sup>4</sup>, Mireille Hontebeyrie<sup>5</sup>, Mariano J. Levin<sup>3</sup>, Cristian R. Smulski<sup>3,4\*</sup>

**1** Unité d'Immunologie Structurale, Institut Pasteur, Paris, France, **2** Centre National de la Recherche Scientifique, Unité de Recherche Associée 2185, Paris, France, **3** Laboratorio de Biología Molecular de la Enfermedad de Chagas, INGENI-CONICET, Buenos Aires, Argentina, **4** UPR9021 du CNRS, Strasbourg, France, **5** Institut Pasteur, Paris, France

## Abstract

Patients with Chronic Chagas' Heart Disease possess high levels of antibodies against the carboxyl-terminal end of the ribosomal P2 $\beta$  protein of *Trypanosoma cruzi* (TcP2 $\beta$ ). These antibodies, as well as the murine monoclonal antibody (mAb) 17.2, recognize the last 13 amino acids of TcP2 $\beta$  (called the R13 epitope: EEEDDDMGFGLFD) and are able to cross-react with, and stimulate, the  $\beta$ 1 adrenergic receptor ( $\beta$ 1-AR). Indeed, the mAb 17.2 was able to specifically detect human  $\beta$ 1-AR, stably transfected into HEK cells, by flow cytometry and to induce repolarisation abnormalities and first degree atrioventricular conduction block after passive transfer to naïve mice. To study the structural basis of this cross-reactivity, we determined the crystal structure of the Fab region of the mAb 17.2 alone at 2.31 Å resolution and in complex with the R13 peptide at 1.89 Å resolution. We identified as key contact residues on R13 peptide Glu3, Asp6 and Phe9 as was previously shown by alanine scanning. Additionally, we generated a model of human  $\beta$ 1-AR to elucidate the interaction with anti-R13 antibodies. These data provide an understanding of the molecular basis of cross-reactive antibodies induced by chronic infection with *Trypanosoma cruzi*.

**Citation:** Pizarro JC, Boulot G, Bentley GA, Gómez KA, Hoebeke J, et al. (2011) Crystal Structure of the Complex mAb 17.2 and the C-Terminal Region of *Trypanosoma cruzi* P2 $\beta$  Protein: Implications in Cross-Reactivity. *PLoS Negl Trop Dis* 5(11): e1375. doi:10.1371/journal.pntd.0001375

**Editor:** Helton da Costa Santiago, National Institutes of Health, United States of America

**Received:** June 18, 2011; **Accepted:** September 11, 2011; **Published:** November 1, 2011

**Copyright:** © 2011 Pizarro et al. This is an open-access article distributed under the terms of the Creative Commons Attribution License, which permits unrestricted use, distribution, and reproduction in any medium, provided the original author and source are credited.

**Funding:** This work was supported by the Pasteur Institute, Paris; Agencia Nacional de Promoción Científica y Tecnológica, Argentina (ANPCyT; BID 1728/OC-AR PICT N° 25845) and Consejo Nacional de Investigaciones Científicas y Técnicas (CONICET), Argentina. Support of CNRS-CONICET and INSERM-CONICET collaborative French-Argentinean research grants, as well as the ECOS-Sud project "Anticorps Anti-Proteines Ribosomales P de *T. cruzi* comme Inhibiteur Spécifique de la Traduction" (France-Argentine, 2005–2008) are acknowledged. The funders had no role in study design, data collection and analysis, decision to publish, or preparation of the manuscript.

**Competing Interests:** The authors have declared that no competing interests exist.

\* E-mail: c.smulski@unistra.fr

‡ Current address: Structural Genomic Consortium (SGC), University of Toronto, Toronto, Canada

## Introduction

*Trypanosoma cruzi*, the etiological agent of Chagas' disease, affects approximately 10–12 million people from different endemic regions in Latin America [1], killing more than 15,000 each year [2,3]. It is also carried by hundreds of thousands of people in Europe (especially Spain and Portugal), the United States, Canada, Japan and Australia, mostly by Latin American immigrants. Accordingly, infection control of blood banks has been recently implemented outside endemic regions [4]. Chagas' disease shows a variable clinical course, which ranges from an acute phase, with parasitemia and asymptomatic features, to serious chronic symptomatic stages characterized by low or no parasitemia, positive serology and involving clinical cardiac, gastrointestinal or neurological disorders [3,5]. The cardiac form, referred as chronic Chagas' heart disease (cChHD), is not only the most frequent and severe consequence of the chronic infection by *T. cruzi*, but is also the main cause of cardiomyopathy in South and Central America [6]. Among other clinical features, cChHD is an arrhythmogenic cardiomyopathy with high prevalence of right

bundle branch block, left anterior hemi block, sinus node dysfunction and complex supraventricular arrhythmias [7,8]; mega disorders of colon or esophagus and neurological disorders are less frequent (around 5% of the infected people) [9,10]. To date, the mechanisms of the pathophysiology of Chagas' disease are not completely understood and two main hypotheses have been proposed: the first is based on the essential role of the parasite in tissular damage while the second argues for an auto reactive process resulting from an impaired immune response associated with molecular mimicry [11,12,13]. Different experimental approaches have shown that both mechanisms may be involved in the chagasic pathology because of the persistence of the parasite in chronic phase [14] and of the presence of parasite antigens carrying epitopes common to host molecules [15].

In 1989, Levin et al. selected and cloned the first parasite molecule, called JL5, presenting a molecular mimicry of a human molecule, using serum from a chronically infected person with cChHD [16,17]. The fine epitope recognized by patients with cChHD was located at the C-terminal end of the *T. cruzi* ribosomal P2 $\beta$  protein (TcP2 $\beta$ ) and was named R13

## Author Summary

*Trypanosoma cruzi* is a protozoan parasite responsible for Chagas disease. Chronic Chagas' heart disease (cChHD) is not only the most frequent and severe consequence of the chronic infection by *T. cruzi*, but is also the main cause of cardiomyopathy in South and Central America. Patients with cChHD possess high levels of antibodies against the carboxyl-terminal tail of the ribosomal P proteins of *T. cruzi* (called the R13 epitope). These antibodies, as well as the murine monoclonal antibody (mAb) 17.2, are able to cross-react with, and stimulate, the  $\beta_1$  adrenergic receptor ( $\beta_1$ -AR). Indeed, the mAb 17.2 was able to specifically detect human  $\beta_1$ -AR and induce some of the classical cardiac symptoms after passive transfer to mice. To study the structural basis of this cross-reactivity, we determined the crystal structure of the Fab region of the mAb 17.2 alone and in complex with R13. Additionally, we generated a model of human  $\beta_1$ -AR to elucidate the interaction with anti-R13 antibodies in order to understand the molecular basis of cross-reactive antibodies induced by chronic infection with *T. cruzi*.

(EEEDDDMGFGLFD) [15,18,19,20]. This highly antigenic acidic epitope bears similarity to an acidic motif (AESDEA) on the second extracellular loop of cardiac  $\beta_1$ -adrenergic receptor ( $\beta_1$ -AR) [21,22]. In addition, a significant correlation between the high level of anti-R13 antibodies (Abs) and ventricular arrhythmias was observed [23], consistent with the hypothesis that R13-specific anti-TcP2 $\beta$  Abs are able to cross-react with and stimulate the  $\beta_1$ -AR [19,20,21,22,23,24,25]. Alanine-mutation scanning experiments on the R13 epitope using different immuno-purified anti-R13 Abs illustrated the complexity of the anti-R13 humoral response since each of the eight anti-R13 Ab preparations presented a unique epitope recognition pattern [23]. Despite this extreme heterogeneity, it was possible to determine a common reactivity profile where Glu3, and to a lesser extent, Asp6 and Phe9 were essential [23]. Indeed, the C-terminal end of the human ribosomal P proteins has one single amino acid change in the third residue (Glu3Ser), a change that diminished the affinity of mAb 17.2 for the corresponding mammalian peptide by about two orders of magnitude [22].

Mice immunized with different recombinant TcP2 $\beta$  proteins (GST or His fusion proteins) and different adjuvants (CFA or ALU) induced a diverse response along the protein sequence. Strikingly, Abs from infected animals recognized only the C-terminal region of the protein (R13 epitope). These different antiserum showed that only Abs specific for the C-terminus were able to increase the beating frequency of cardiomyocytes from neonatal rats *in vitro* by selective stimulation of the  $\beta_1$ -AR [24]. These immunization data led to protocols for the production of a monoclonal antibody directed against the R13 epitope, the mAb 17.2. This mAb was demonstrated to i) recognize a linear epitope of the C-terminal end of TcP2 $\beta$  protein (R13), ii) react with peptides derived from the second extracellular loop of the human  $\beta_1$ -AR, iii) induce a dose-dependent increase on the beating frequency of cardiomyocytes in culture that is abolished by bisoprolol, a specific  $\beta_1$ -AR antagonist [22], and iv) provoke apoptosis in murine cardiac cell lines, HL-1 [26].

In the present work, we report the three-dimensional structure of the Fab fragment of mAb 17.2 determined by X-ray crystallography, alone and in complex with its cognate peptide epitope, providing a description of structural changes that occur upon binding the antigen. The mAb 17.2 was shown by flow

cytometry to specifically detect HEK cells transfected with the human  $\beta_1$ -AR. In addition, passive transfer to naive mice induced some of the classical symptoms of the Chagasic cardiomyopathy, such as repolarisation abnormalities and first degree atrioventricular (AV) conduction block. Finally, we discuss the relationship between epitope mimicry and bystander activity of anti-R13 Abs on the  $\beta_1$ -AR using our crystal structure of the Fab 17.2 in complex with a model of the human  $\beta_1$ -AR constructed from the turkey  $\beta_1$ -AR structure that was recently determined [27].

## Materials and Methods

### 1. Ethics statement

The research was conducted in accordance with the European Community guidelines for use of experimental animals. The IBMC animal house facilities are approved by French veterinary service (#E67-482-2). No surgery has been done on animals. Mice were euthanized according the European Community guidelines.

### 2. Preparation and purification of mAb 17.2

The mAb 17.2 (isotype IgG1,  $\kappa$ ) was obtained by immunizing BALB/c mice with recombinant TcP2 $\beta$  [22]. The mAb was purified from ascitic fluid by precipitation with 40% ammonium sulphate at pH 7.4, followed by ion-exchange chromatography on a DEAE-Sephacel (Pharmacia, Sweden) column equilibrated in 17.5 mM NaCl at pH 8.0. The elution was done with 40 mM NaCl at pH 8.0. The sample was then dialyzed against 0.1 M potassium phosphate at pH 7.2.

After addition of 5 mM  $\beta$ -mercaptoethanol and 2.5 mM EDTA, the IgG was treated with papain at an enzyme:substrate ratio of 1:100 at 37°C for 2 h. The reaction was stopped by addition of iodacetamide (1 mg/ml) before dialysis against 10 mM sodium phosphate at pH 8.0. The Fab was then added to a DEAE-Sephacel (Pharmacia, Sweden) column equilibrated with the same buffer. Fab 17.2 was eluted with phosphate buffer and then concentrated on a Centricon 10.

### 3. Synthetic peptide

R13 peptide (EEEDDDMGFGLFD, representing the C-terminal region of TcP2 $\beta$ ) was synthesized by the solid-phase method of Merrifield [28], with a semi-automatic multi-synthesizer NPS 4000 (Neosystem, France).

### 4. Crystallization of the complex Fab 17.2

Crystals of apo Fab 17.2 and its complex with R13 were grown by vapour diffusion using the hanging drop technique. One volume of Fab 17.2 at 10 mg/ml was mixed with one volume of a solution consisting of 18% (w/v) PEG 8000, 0.1 M sodium cacodylate at pH 6.7, 0.2 M calcium acetate, 12.5 mM Tris-HCl pH 7.5 and 25 mM NaCl. The drop, with a final protein concentration of 4.2 mg/ml, was sealed over a reservoir containing 1 ml of mother liquor. Crystallization of the Fab 17.2/R13 peptide was performed under the same conditions as above with Fab and peptide concentrations of 15 mg/ml and 10 mg/ml, respectively, giving an Ab/antigen molar ratio  $\sim 1/20$ .

### 5. Crystallographic data and structure solution

Diffraction data were collected on the beam lines ID14-1 (Fab 17.2/R13 complex) and BM30A (apo Fab 17.2) at the European Synchrotron Radiation Facility, Grenoble, France. The two crystal forms belong to space group P2<sub>1</sub> with very similar unit cell parameters. Diffraction data were integrated and scaled using the programs HKL and SCALEPACK [29]. The structure was solved by molecular replacement with the program AMoRe [30],

using antibody variable and constant dimers derived from PDB entry 2igf as search models. Two independent Fab molecules, expected from the unit cell volume, were readily located and the structure was refined using the program autoBUSTER (Global Phasing Ltd.). Manual adjustments between refinement runs and building of the R13 peptide in the complex were performed with the program COOT [31]. Crystallographic parameters, diffraction data statistics and structure refinement results are summarized in Table 1.

## 6. $\beta$ 1-AR competition binding experiments

HEK cells and HEK cells transfected with  $\beta$ 1-AR (HEK- $\beta$ 1) were cultured in DMEM (GIBCO, Invitrogen, USA) with 10% FCS, 100 U/ml penicillin, 100 mg/ml streptomycin and 2 mM L-glutamine, using 200  $\mu$ g/ml hygromycin B (Sigma, USA) for transfected cell maintenance [25].

HEK and HEK- $\beta$ 1 cells were seeded in FACS tubes at  $8 \times 10^5$  cell/ml and incubated with mAb 40.14 or 17.2 (500 nM) or with mAb 17.2 (500 nM) pre-incubated for 2 h at 37°C with 10  $\mu$ M R13 peptide in supplemented DMEM. After 1 h at room temperature, cells were stained with Cy3-conjugated goat anti-mouse IgG (Jackson ImmunoResearch, USA) and propidium iodide (PI) to exclude the dead cell population. Cells were detected using a BD FACSARIA flow cytometer (BD Biosciences) and results were analysed with WinMdi 2.9 software (Copyright 1993–2000 Joseph Trotter). Values are expressed as means  $\pm$  S.D. ( $n = 3$ ) and statistical comparisons were performed using One-way and Two-way ANOVA with Bonferroni's Multiple Comparison post test using GraphPad Prism version 5.00 for Windows, GraphPad Software, San Diego California USA, www.graphpad.com.  $P < 0.05$  was considered statistically significant.

## 7. Electrocardiogram recordings

Three female BALB/c mice, 20 g each, were anesthetized using intraperitoneal Tribromoethanol 150 mg/Kg. The mAb 17.2 was injected intravenously at 200 nM in 200  $\mu$ l of saline solution (0.9% NaCl). Electrocardiogram (ECG) recordings were performed during 30 min after injection. ECGs were obtained with the six standard leads (I, II, III, AVR, AVL, AVF) at 50 mm/s of paper speed and at 20 mm/mV amplitude using a Fukuda-Denshi Fx-2111 electrocardiograph (Tokyo, Japan) [32]. Electrocardiographic analysis included measurements of heart rate, P wave duration and amplitude, QRS complex duration and amplitude, P-R interval duration and a search for disturbances of rhythm, conduction, and repolarisation.

## 8. Molecular modelling

All procedures were performed with Discovery Studio 2.5 software from Accelrys (San Diego, CA, USA). The crystal structure of the turkey  $\beta$ 1-AR (PDB 2VT4) was used as template to build a model of the human  $\beta$ 1-AR. We mutated all residues to the human sequence and optimized the conformation of both the mutated residues and any surrounding residues that lay within a cut-off radius of 2 Å. Five models thus obtained were scored by the Discrete Optimized Protein Energy (DOPE). We continued analysis using the lowest energy model (DOPE =  $-39358.55$  kcal/mol), which was superimposed onto a membrane model. The R13 epitope structure was aligned with the second extracellular loop of the humanized  $\beta$ 1-AR model to allow positioning of the Ab on the putative cross-reactive epitope. Once the Ab was positioned, a fixed atom constraint was applied to the whole  $\beta$ 1-AR with the exception of the extracellular regions and a harmonic restraint was applied to the framework regions of the Ab. Finally, the complex was subjected to an initial minimization step (max 500), RMS gradient 0.1 Kcal/mol by conjugated gradient; followed by a second minimization step (max 500), RMS gradient 0.0001 Kcal/mol by conjugated gradient. The structure was then submitted to a dynamic simulation including heating (2000 steps), equilibration (1000 steps) and production (1000 steps) at 300 °K with a time step of 0.001 ps under a distance-dependent, dielectric constant, implicit solvent model. A negative intermolecular energy of  $-430$  kcal/mol was obtained for the complex under these conditions. All images were generated using PyMOL Molecular Graphics System, Version 1.0, Schrödinger, LLC.

## Results

### Structure of apo Fab 17.2 and its complex with R13

We determined the crystal structure of the Fab region of the mouse monoclonal antibody 17.2, in the apo form and in complex with the peptide R13 (EEEDDDMGFGLFD), corresponding to the C-terminal epitope of TcP2 $\beta$ . The asymmetric unit of both crystal structures contains two independent apo Fab molecules or Fab-R13 complexes (referred as molecule 1 and 2). The N- and C-termini of R13 show considerable mobility and only the first eleven amino acid residues (EEEDDDMGFGL) in both complexes could be traced in the electron density maps. The two independent Fab molecules of each crystal form show small differences in quaternary structure, as revealed by the difference in elbow angle (angle subtended by the pseudo two-fold axes of the variable and constant dimers). The Fab 17.2 elbow angles are 152/144° and 150/146° for the apo and R13 complex, respectively (molecule1/molecule2), and lie within the range of previously reported values [33]. These reflect the different lattice environments of the two independent molecules in the asymmetric unit since the respective

**Table 1.** Crystallographic data and refinement statistics.

Space group	Fab 17.2 - R13 (EEEDDDMGFGLFD)		Fab 17.2 apo	
	P2 <sub>1</sub>	P2 <sub>1</sub>	P2 <sub>1</sub>	P2 <sub>1</sub>
Cell parameters	a	83.00	82.07	
	b	68.21	65.68	
	c	92.11	91.37	
	(Å)			
	$\beta$ (°)	98.4	98.2	
Resolution (Å)	30.0–1.89	1.94–1.89	30.0–2.29	2.34–2.29
Total reflections	282283		144,460	2210
Unique reflections	73,918	3090	41,572	1458
R <sub>merge</sub>	0.077	0.405	0.049	0.170
Completeness (%)	92.0	57.9	94.6	50.7
$\delta$	14.6	2.7	22.9	4.2
Redundancy	3.82	3.82	3.47	3.47
B Wilson (Å <sup>2</sup> )	28.8		28.8	
Refinement				
Resolution (Å)	20.0–1.89	1.94–1.89	20.0–2.31	2.37–2.31
R <sub>factor</sub>	0.1795	0.2107	0.1724	0.2013
R <sub>free</sub>	0.2178	0.2459	0.2355	0.3122
rms bonds (Å)	0.010		0.010	
rms angle (°)	1.15		1.25	

doi:10.1371/journal.pntd.0001375.t001

elbow angles for molecules 1 and 2 are common to both crystal forms, which are closely isomorphous.

No significant structural differences were observed between individual variable domains. A pair-wise superposition of all VL domains from the apo and R13 complex Fab molecules gives a mean r.m.s. difference in C $\alpha$  position of 0.28 Å (range 0.23–0.34 Å). Similarly, the superimposed VH domains give a mean r.m.s. difference in C $\alpha$  positions of 0.28 Å (range 0.23–0.33 Å). For both VH and VL, the largest differences occur between the R13 complex and apo forms, but these are small, showing that the polypeptide conformation was largely conserved upon binding the antigen. The most notable structural change to occur upon binding R13 is a small relative rotation between the VL and VH domains, leading to an opening out at the antigen-binding site when the antigen is bound, with a 4.2° rotation from the apo to R13 complex state for molecule 1 and 4.6° for molecule 2. The distance between the tips of CDR-L1 and CDR-H2 is correspondingly shifted from 15.7 Å and 16.8 Å in the apo structure to 18.9 Å and 18.2 Å in the R13 complex in molecules 1 and 2, respectively (**Figure 1**). Interestingly, side chain conformations at the antigen binding site are entirely conserved upon binding the antigen (**Figure 2A**). In addition, there are six water molecules within the Fab 17.2 antigen combining site in the apo structure that are displaced by the peptide in the Fab 17.2 R13 complex (**Figure 2B**). Two of the water molecules in the apo structure are replaced by the side chains of Glu3 and Asp6, supporting the pivotal role of these residues in the antibody-

antigen interaction. The remaining four waters are displaced by the main chain of the peptide, residues Met7 to Gly10 (**Figure 2C**). The complex structure also reveals two water-mediated interactions between the peptide and the CDR-H1 (Thr31 and Asn32) engaging both side and main chain atoms of a single epitope residue, Asp4.

The two bound R13 peptides from the complexes in the asymmetric unit are similar in structure, superimposing with an r.m.s. difference in C $\alpha$  positions of 0.78 Å (1.06 Å for all main chain atoms). The peptide structures diverge most at the N- and C-termini, where contacts with the antibody are sparse, but are very similar in the central region of the peptide between residues Asp3 and Gly10 (**Figure 2D**). Antibody-peptide interactions are similar in the two independent Fab 17.2-R13 complexes and include 13 hydrogen bonds, four with VL and nine with VH, as well as a salt bridge between VH Arg52 and R13 Glu3 (**Table 2**). In addition, an aromatic stacking interaction occurs between VL Tyr101 and R13 Phe9. These results highlight the importance of some key contact residues on the epitope, such as Glu3, Asp6 and Phe9 (**Figure 2E**).

### Functional activity of the mAb 17.2

The cross-reaction of anti-R13 Abs with  $\beta$ 1-AR has been extensively reported [22,23,24,34]. Indeed, the mAb 17.2, first described by Mahler et al (2001) [22], induced a dose-dependent increase on the beating frequency on neonatal rat cardiomyocytes culture that was abolished by bisoprolol, a specific  $\beta$ 1-AR

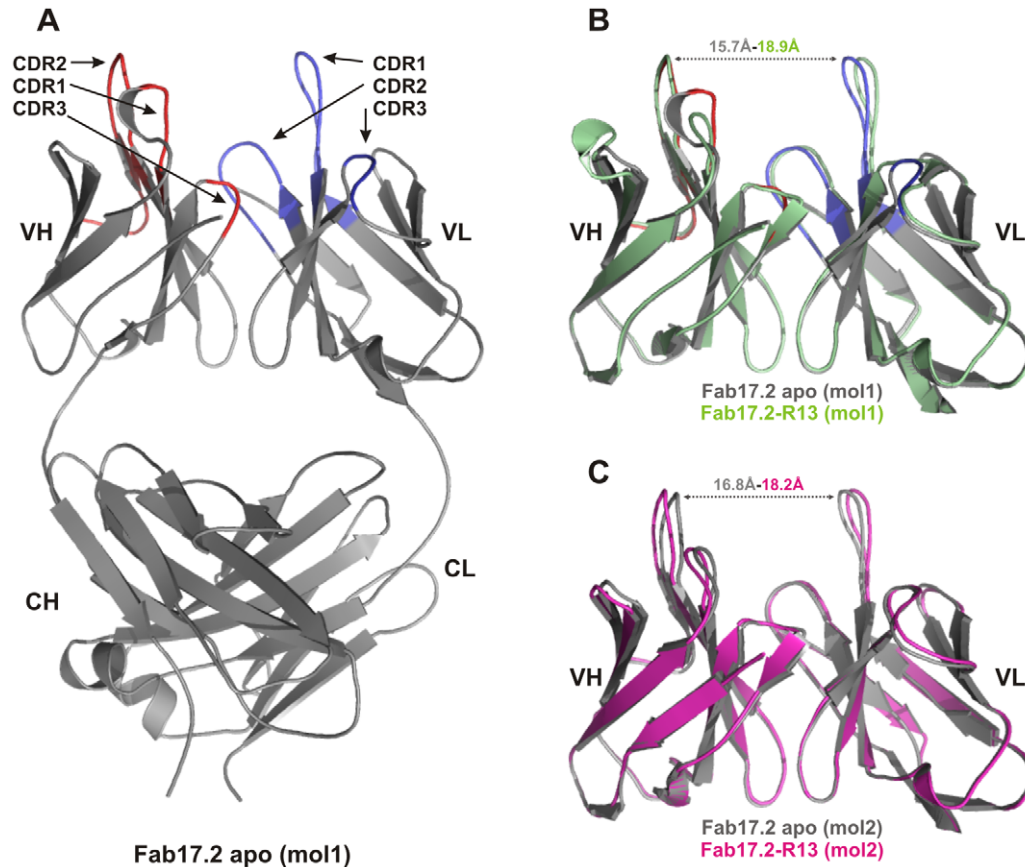


**Figure 1. Structure of the Fab 17.2.** A. Apo Fab 17.2 structure (molecule 1). Heavy chain CDRs are coloured in red and light chain CDRs in blue. B. Superposition of molecules 1, VH-VL region of the two crystals asymmetric units. C. Superposition of molecules 2, VH-VL region of the two crystals asymmetric units. Apo Fab 17.2 (grey), Fab 17.2-R13 molecule 1 (green) and molecule 2 (magenta). doi:10.1371/journal.pntd.0001375.g001

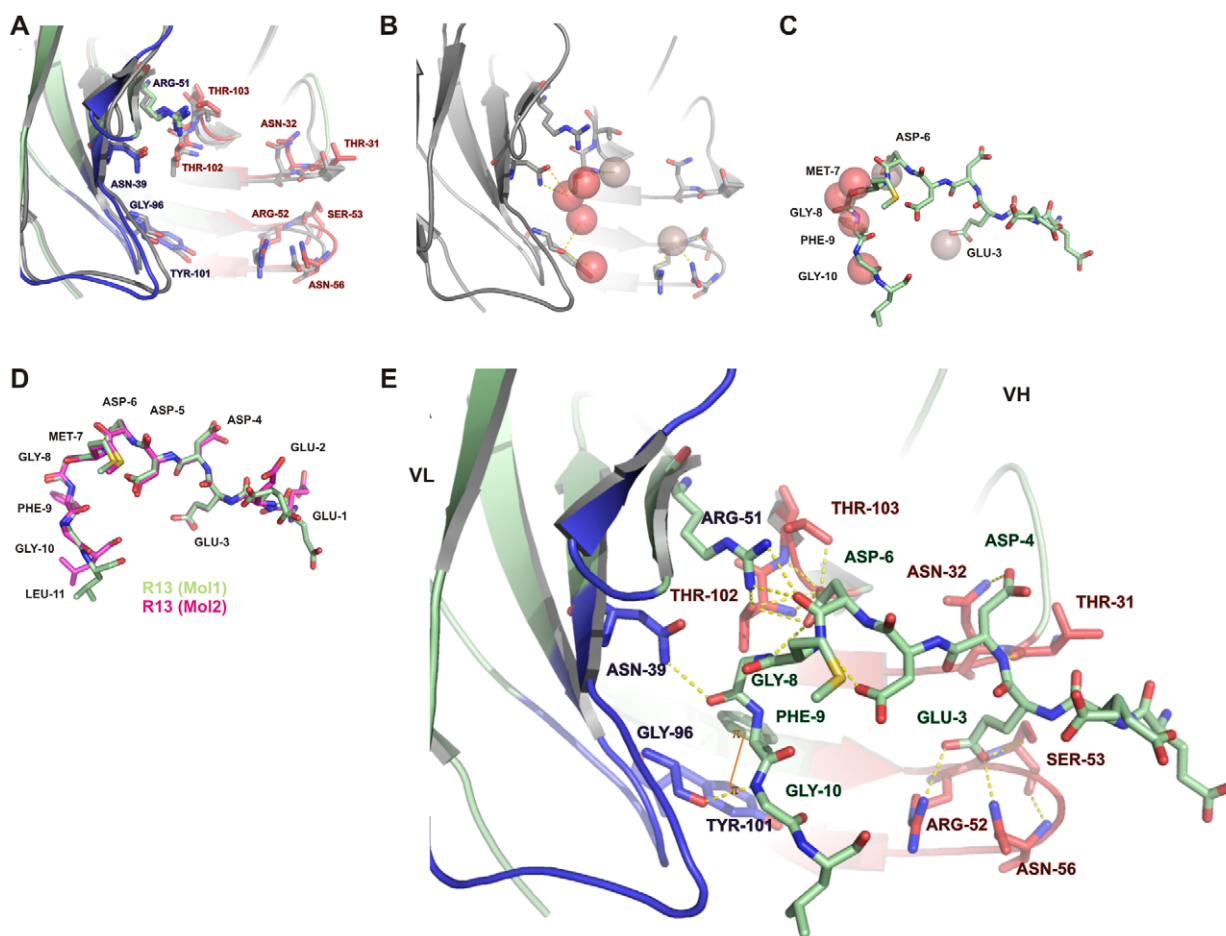


**Figure 2. Structure of the Fab17.2 – R13 complex.** A. Superposition of the apo Fab 17.2 and R13 complex structures (grey and green respectively). VH and VL contact residues are indicated. B. Main water molecules present on the antigen binding site of Fab 17.2 apo. C. Superposition of water molecules present on the antigen binding site of Fab 17.2 apo that are replaced by the peptide in the Fab 17.2 R13 complex. D. Superposition of R13 peptides from molecules 1 (green) and 2 (magenta). E. Structure of the Fab 17.2-R13 complex (molecule 1). All hydrogen bonds between mAb 17.2 and peptide R13 are illustrated as dotted yellow lines. The  $\pi$ -stacking interaction between VL Tyr101 and the epitope Phe9 is also indicated. Heavy chain CDRs are coloured in red and light chain CDRs in blue the peptide is coloured in light green.

doi:10.1371/journal.pntd.0001375.g002

**Table 2. Polar contacts between Fab 17.2 and R13 peptide.**

Fab	CHAIN	CDR	Atom [MC/SC]	...	O [MC]	Ag
Asn39	L	1	N $\delta$ 2 [SC]	...	O [MC]	Gly8
Arg51	L	2	N $\eta$ 2 [SC]	...	O [MC]	Asp6
Arg51	L	2	N $\eta$ 1 [SC]	...	O [MC]	Asp6
Gly96	L	3	O [MC]	...	N [MC]	Gly10
Thr31	H	1	O [MC]	...	N [MC]	Asp4
Asn32	H	1	N $\delta$ 2 [SC]	...	O $\delta$ 1 [SC]	Asp4
Arg52	H	2	N $\eta$ 1 [SC]	...	O $\epsilon$ 2 [SC]	Glu3
Ser53	H	2	N [MC]	...	O $\epsilon$ 1 [SC]	Glu3
Ser53	H	2	O $\gamma$ [SC]	...	O $\epsilon$ 1 [SC]	Glu3
Asn56	H	2	N $\delta$ 2 [SC]	...	O $\epsilon$ 1 [SC]	Glu3
Thr102	H	3	N [MC]	...	O $\delta$ 2 [SC]	Asp6
Thr102	H	3	O $\gamma$ 1 [MC]	...	O $\delta$ 1 [SC]	Asp6
Thr103	H	3	N [MC]	...	O $\delta$ 2 [SC]	Asp6
Thr103	H	3	O $\gamma$ 1 [SC]	...	O $\delta$ 2 [SC]	Asp6

MC: Main Chain; SC: Side Chain.

doi:10.1371/journal.pntd.0001375.t002

antagonist. Here, we show by flow cytometry that mAb 17.2 specifically recognized human  $\beta$ 1-AR presented in a stable HEK- $\beta$ 1 cell line (**Figure 3A and B**). This cell line possesses a high receptor expression (800–1300 fmol/mg of total protein), as has been previously reported [35]. The mAb 40.14, which recognizes an internal epitope on TcP2 $\beta$ , gave no signal, indicating the specificity of mAb 17.2- $\beta$ 1-AR interaction (**Figure 3B**). In addition, this interaction was inhibited by pre-incubation of the mAb 17.2 with R13 peptide (**Figure 3B inset**). Furthermore, passive transfer of mAb 17.2 to naïve mice induced an increase in the beating rate from 240 bpm to 300 bpm after 30 minutes (**Figure 3C**). Repolarisation abnormalities (a) and first degree AV conduction block (b) were recorded at 15 and 30 minutes post-injection.

#### Modelling the interaction with the human $\beta$ 1-AR

In view of the functional activity of the Ab on  $\beta$ 1-AR, we generated a model of the interaction of the Fab 17.2 with the human receptor from the crystal structure of the turkey homologue. Briefly, we generated a model of the human  $\beta$ 1-AR as described under material and methods. The structure of TcP2 $\beta$  epitope, R13, was aligned to the humanized second extracellular

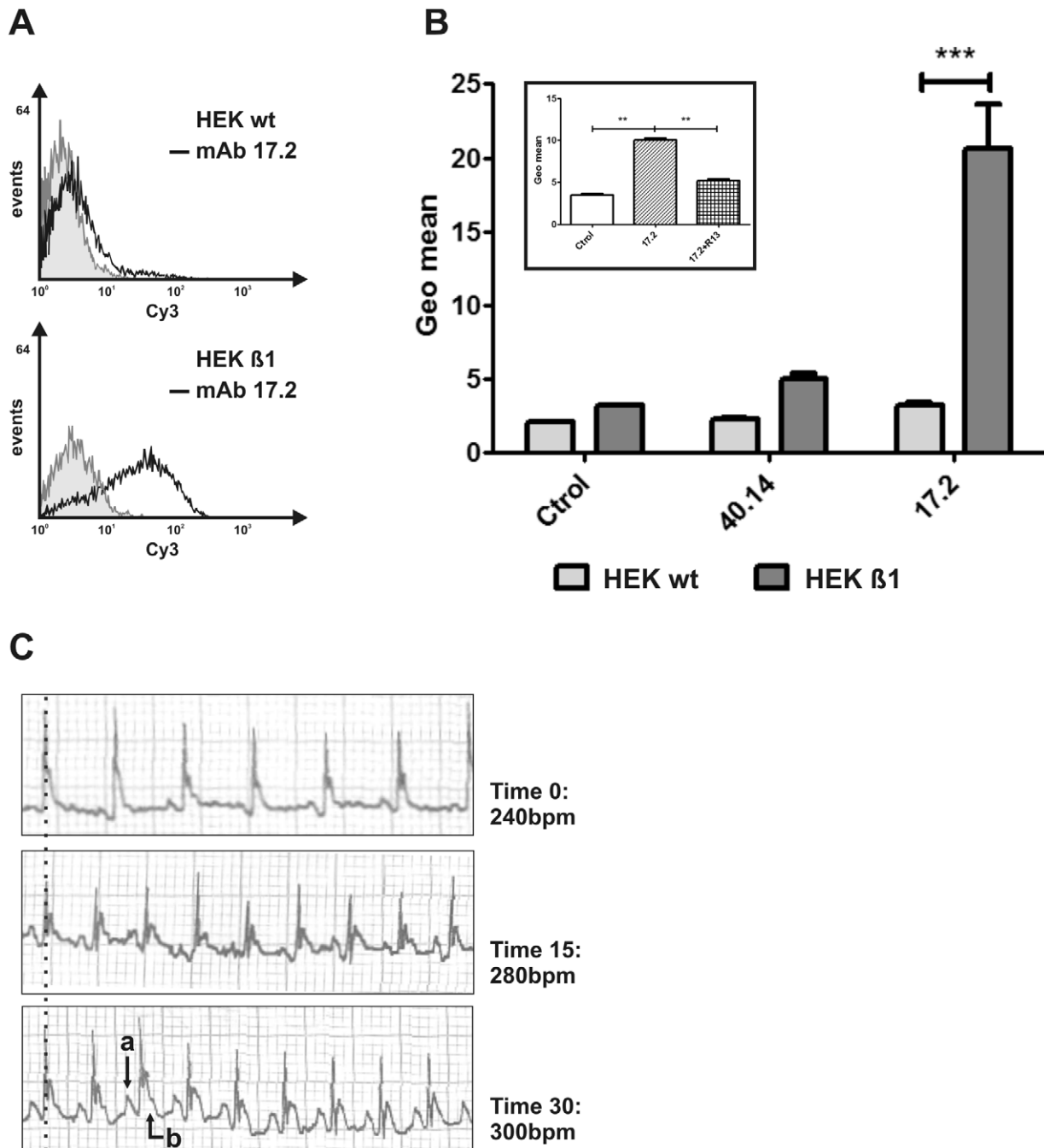


**Figure 3. Functional activity of the mAb 17.2.** A. Representative histogram showing the HEK and HEK- $\beta$ 1 cells labelled with mAb 17.2 followed by a Cy3-conjugated goat anti-mouse IgG. B. Results are expressed as means  $\pm$  SD (n=3). Inset: Binding of mAb 17.2 to HEK- $\beta$ 1 cells in the presence of R13 peptide. \*\*  $p < 0.01$ ; \*\*\*  $p < 0.001$ . C. Passive transfer of mAb 17.2 to naïve mice. Repolarisation abnormalities (a) and first degree AV conduction block (b) are indicated by arrows. bpm: beats per minute. doi:10.1371/journal.pntd.0001375.g003

loop (2ECL) of the model to allow positioning the Ab on the putative binding site (Figure 4A) and the complex was subjected to a two minimization steps followed by heating, equilibration and production protocols under a distance-dependent, dielectric-implicit solvent model (Figure 4B). The interaction energy of the complex Ab- $\beta$ 1-AR was estimated at  $-430$  kcal/mol. Polar contacts found in the model are summarized in Table 3. Some of Ab residues identified in the interaction with the humanized 2ECL peptide were key residues in the interaction with the *T. cruzi*

epitope, such as Thr31, Arg52 and Asn56 of the heavy chain. In addition, the acidic residues present on the humanized  $\beta$ 1-AR model (Asp187, Glu188, Asp195 and Asp200) established many hydrogen bonds with different residues of the Fab (Figure 4C). Remarkably, while the light chain established just a few contact points with the *T. cruzi* epitope, it established many hydrogen bonds with  $\beta$ 1-AR, as can be seen in Figure 4 and Table 3, suggesting an important role in stabilizing the interaction with the receptor.

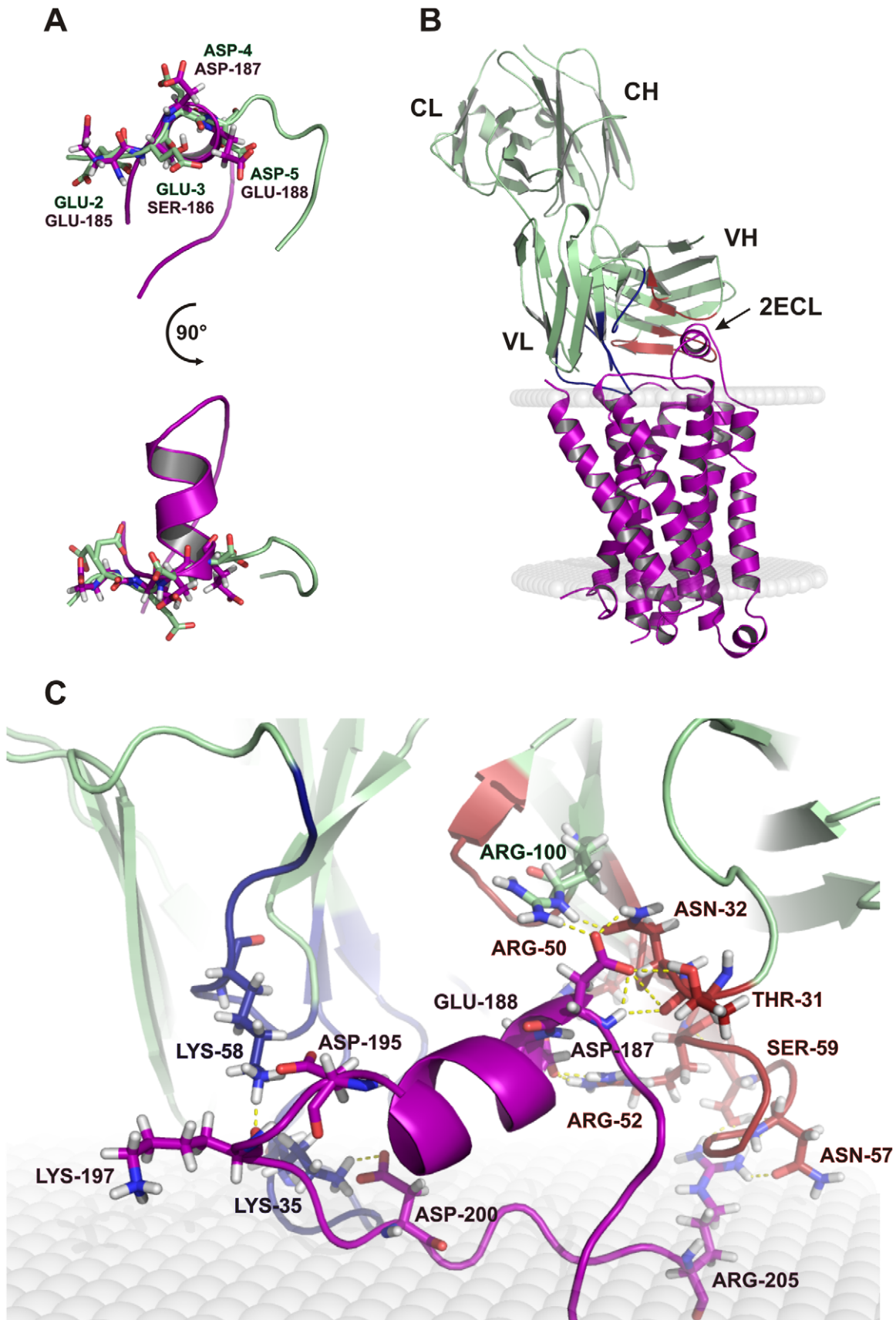


**Figure 4. Model of the interaction of Fab 17.2 with the human  $\beta$ 1-AR.** A. Superposition of the second extracellular loop (2ECL) of the human  $\beta$ 1-AR model (violet) and the region 2–5 of the epitope (light green). B. Complex of the Fab 17.2 (light green) with the human  $\beta$ 1-AR (violet) inserted in a membrane model (grey). C. Zoom of the paratope region of 17.2 interacting with the second extracellular loop. The main contact points are illustrated as dotted yellow lines. Heavy chain CDRs are coloured in red and light chain CDRs in blue.  
doi:10.1371/journal.pntd.0001375.g004

## Discussion

Alanine-mutation scanning analysis on the R13 epitope showed the importance of Glu3, Asp5, Asp6, Gly8 and Phe9 for mAb 17.2 recognition [22]. Crystal structure confirmed the interaction of Glu3, Asp6, Gly8 and Phe9 with the antibody and exposed a polar contact between Asp5 and Met7. This interaction may contribute to stabilize the conformation of the peptide that was shown to behave as random coil in solution [36].

Despite the sequence similarity between the epitope sequence (EEEDDDMGFGL) of TcP2 $\beta$  and the acidic region on the human second extracellular loop (AESDEA) of  $\beta$ 1-AR, crystallographic data and modelling showed that this minimal region is involved but not sufficient for an effective interaction. The interaction energy between the Fab and the whole receptor was estimated at  $-430$  kcal/mol. However, the interaction energy of the Ab with only the 2ECL was  $-283$  kcal/mol, suggesting that other regions on the receptor contribute to stabilize the interaction within the complex. These data could also explain the low affinity of mAb 17.2, or single chain derived recombinant antibodies, with the  $\beta$ 1-AR 2ECL peptide H26R measured by surface plasmon

resonance [22,25]. It is possible that electrostatic forces guide the first contacts between an electropositive antigen-binding pocket and the electronegative region of the 2ECL, with the heavy and light chains establishing additional contacts with the receptor. Comparison of the buried surfaces in both crystallized complex and the model (**Table 4**) shows a larger surface for the complex with the  $\beta$ 1-AR, supporting this hypothesis. However, the shape complementarities for the model-Fab complex were smaller in comparison to R13 complex (**Table 4**), suggesting a reduced affinity for the  $\beta$ 1-AR. Together, these data support the idea of a bystander activity of mAb 17.2 on the cardiac receptor rather than classical epitope mimicry of acidic residues.

Recently, the crystal structure of turkey  $\beta$ 1-AR in complex with different agonists and antagonists was published [37]. In this work, the authors showed the presence of structural differences between the 2ECL of the  $\beta$ 1-AR bound to the agonist dobutamine (PDB 2Y01) and to the antagonist cyanopindolol (PDB2VT4). A 1 Å contraction of the ligand-binding pocket between helices H5 and H7 was observed in the agonist complex relative to the antagonist complex. The contraction of the catecholamine-binding pocket induced a conformational change in the 2ECL [37]. In addition, we previously reported the construction of two single chain recombinant antibodies (scFv) derived from the mAb 17.2, named scFv C5 and B7 [25]. Both scFv were able to recognize *T. cruzi* ribosomal P proteins and  $\beta$ 1-AR in Western blot, ELISA, surface plasmon resonance and immunofluorescence. In functional assays, however, the monomeric scFv B7 behaved as a  $\beta$ 1-AR antagonist, while the dimeric scFv C5 acted as a  $\beta$ 1-AR agonist. The interaction of the Fab fragment with the  $\beta$ 1-AR should thus correspond to an antagonist conformation. A dimeric interaction of the Ab with the receptor would, however, be constrained by the distance of the two antigen-binding sites on the dimeric Ab. Since  $\beta$ 1-AR forms a family of dimeric membrane proteins, we suggested that the interaction constraints between the two dimers require a small rearrangement of the receptor dimer, decreasing the pharmacophore pocket, as has been described for partial agonists [37]. This could explain the experimental observation that monomeric fragments of Abs against the second extracellular loops of  $\beta$ 1-AR act as inverse agonists while the bivalent fragments or dimeric antibodies behave as partial agonists [25,38,39,40].

**Table 3. Polar contacts in the model between 17.2 and  $\beta$ 1-AR.**

mAb	CHAIN	CDR	Atom [MC/SC]			$\beta$ -1AR
Gln27	L	1	O $\epsilon$ 1 [SC]	...	H $\eta$ 22[SC]	Arg323
Ser28	L	1	O $\gamma$ [SC]	...	H $\eta$ 11[SC]	Arg323
Asp31	L	1	O $\delta$ 2 [SC]	...	H $\omega$ [MC]	Arg323
Ser32	L	1	O $\gamma$ [SC]	...	H $\omega$ [MC]	Val326
Lys35	L	1	H $\zeta$ 1 [SC]	...	O $\delta$ 1 [SC]	Asp200
Lys35	L	1	H $\zeta$ 1 [SC]	...	O $\delta$ 2 [SC]	Asp200
Lys35	L	1	H $\zeta$ 2 [SC]	...	O $\delta$ 2 [SC]	Asp200
Lys58	L	2	H $\zeta$ 1 [SC]	...	O [MC]	Lys197
Lys58	L	2	H $\zeta$ 2 [SC]	...	O $\delta$ 1 [SC]	Asp195
Lys58	L	2	H $\zeta$ 3 [SC]	...	O $\delta$ 1 [SC]	Asp195
Lys58	L	2	H $\zeta$ 3 [SC]	...	O $\delta$ 2 [SC]	Asp195
His98	L	3	H $\delta$ 1 [SC]	...	O [MC]	Asp322
Thr31	H	1	H $\gamma$ 1 [SC]	...	O $\delta$ 2 [SC]	Asp187
Asn32	H	1	H $\delta$ 22[SC]	...	O $\delta$ 1 [SC]	Asp187
Arg50	H	2	H $\eta$ 22 [SC]	...	O $\epsilon$ 1 [SC]	Glu188
Arg52	H	2	H $\eta$ 12 [SC]	...	O $\epsilon$ 2 [SC]	Glu188
Arg52	H	2	H $\eta$ 22 [SC]	...	O $\epsilon$ 2 [SC]	Glu188
Asn56	H	2	O $\delta$ 1 [SC]	...	H $\eta$ 11 [SC]	Arg317
Asn57	H	2	O $\delta$ 1 [SC]	...	H $\eta$ 11 [SC]	Arg205
Asn57	H	2	O [MC]	...	H $\eta$ 12 [SC]	Arg205
Ser59	H	2	O $\gamma$ [SC]	...	H $\eta$ 12 [SC]	Arg205
Ser59	H	2	O $\gamma$ [SC]	...	H $\eta$ 22 [SC]	Arg205
Tyr61	H	2	H $\eta$ [SC]	...	O [MC]	Phe315
Arg100	H	3	H $\eta$ 21 [SC]	...	O $\delta$ 1 [SC]	Asp187

MC: Main Chain; SC: Side Chain.

doi:10.1371/journal.pntd.0001375.t003

**Table 4. Buried surface upon complex formation, with shape complementarities (Sc) [50] and number of contacts observed between the mAb 17.2 and the R13 peptide in the crystal structure<sup>1</sup> and the model<sup>2</sup>.**

		Fab17.2 - R13 <sup>1</sup>	Fab17.2 - $\beta$ 1AR <sup>2</sup>
Surface ( $\text{\AA}^2$ )	Ab ( $V_L/V_H$ )	648 (252.7/395.3)	1414.9 (868.3/546.6)
	Ag	845	2972.1
	Total	1493	4387
Sc		0.77	0.614
N $^\circ$ contacts	Polar	14	46
	Total	32	96

doi:10.1371/journal.pntd.0001375.t004

The clinical relevance of auto-reactive Abs in the context of the pathogenesis of cChHD is still controversial. Chronic Chagas' patients develop Abs against G protein-coupled receptors such as  $\beta$ 1-AR,  $\beta$ 2-AR and M2-AChR and there are different profiles of these Abs accordingly with the clinical outcome [23,41,42]. In the case of cChHD, there is a prevalence of  $\beta$ 1-AR and M2-AChR Abs [43]. Interestingly these Abs can be detected before the clinical manifestations, supporting the hypothesis of Abs as pathogenic driver for clinical manifestations such as cardiomyopathy or megacolon [43]. It is well documented that chronic adrenergic stimulation mediated by antibodies may have a cardiotoxic effect resembling that caused by catecholamine, which induce cardiac changes similar to those observed in Chagas' disease; namely induction of micro focal lesions associated with a mononuclear cell infiltrate with increased involvement of the left ventricle, and particularly the left ventricular apex [44,45,46,47,48]. Moreover, IgGs from cChHD patients as well as the monoclonal antibody 17.2 were able to provoke apoptosis on HL-1 cardiac cell line, effect that was diminished by either R13 peptide or propranolol [26], reinforcing the pathogenic role of anti-R13 Abs acting on the  $\beta$ 1-AR.

Our data provide a molecular basis for the understanding of the  $\beta$ 1-AR bystander activation by anti-R13 Abs. Furthermore, as severe cases of chronic Chagas' Heart Disease are related to high levels of Abs directed against the R13 epitope [8,17,18,19,20,23,49], and immuno-purified anti-R13 Abs from some of these patients showed in common that R13 residues Glu3, Asp6 and

Phe9 were essential for recognition [23] (as was shown for mAb 17.2), we suggest that high blood concentrations of these antibodies may exert a systemic effect by inducing functional changes in cell types and tissues expressing this receptor, thereby increasing liability to chronic pathology from *T. cruzi* infection.

## Acknowledgments

We thank Dr. Sylviane Muller and Prof. Sylvie Fournel (UPR 9021 Strasbourg, France) for helpful collaboration in the publication of this article; Maximiliano Juri-Ayub and Josiane Gregoire for production and purification of mAb 17.2 and A. Benatar for his collaboration with FACS experiments. HEK- $\beta$ 1 cells were kindly provided by Dr. Federico Mayor Jr. (Universidad Autónoma de Madrid, Spain). We thank the staff of the European Synchrotron Radiation Facility, Grenoble, France, for providing facilities for diffraction measurements and for assistance.

*In memory of Dr. Mariano J. Levin (1951–2010), Director of the Laboratory of Molecular Biology of Chagas' disease, INGEBI-CONICET, Buenos Aires, Argentina, from 1985 to 2010.*

## Author Information

Coordinates have been submitted to the PDB database under accession codes 3SGD and 3SGE for Fab 17.2 apo and Fab 17.2-R13 complex respectively.

## Author Contributions

Conceived and designed the experiments: GAB MJL MH CRS. Performed the experiments: JCP GB GAB KAG MH CRS. Analyzed the data: JCP GAB KAG JH CRS. Contributed reagents/materials/analysis tools: KAG MJL MH GAB CRS. Wrote the paper: JCP GAB MH CRS.

## References

- Moncayo A, Silveira AC (2009) Current epidemiological trends for Chagas disease in Latin America and future challenges in epidemiology, surveillance and health policy. *Mem Inst Oswaldo Cruz* 104 Suppl 1: 17–30.
- Schofield CJ, Jamnin J, Salvatella R (2006) The future of Chagas disease control. *Trends Parasitol* 22: 583–588.
- (2002) Control of Chagas disease. *World Health Organ Tech Rep Ser* 905: i–vi, 1–109, back cover.
- Hontebeyrie M, Brenière SF, Aznar C (2010) Others forms of transmission in American Trypanosomiasis Chagas disease, One hundred years of research. edited by J Telleria and M Tibayrenc. Elsevier. pp 583–597.
- Rassi A, Jr., Rassi A, Marin-Neto JA. Chagas disease. *Lancet* 375: 1388–1402.
- Rassi A, Jr., Rassi A, Little WC (2000) Chagas' heart disease. *Clin Cardiol* 23: 883–889.
- Elizari MV, Chiale PA (1993) Cardiac arrhythmias in Chagas' heart disease. *J Cardiovasc Electrophysiol* 4: 596–608.
- Chiale PA, Ferrari I (2001) Autoantibodies in Chagas' cardiomyopathy and arrhythmias. *Autoimmunity* 34: 205–210.
- Koberle F (1968) Chagas' disease and Chagas' syndromes: the pathology of American trypanosomiasis. *Adv Parasitol* 6: 63–116.
- Palmieri JR, LaChance MA, Conner DH (1984) Parasitic infection of the peripheral nervous system. In: PJ Dyck, PK Thjomas, EH Lambert, R Bunge, eds. *Peripheral Neuropathy* 2: 1988–2009.
- Kierszenbaum F (1999) Chagas' disease and the autoimmunity hypothesis. *Clin Microbiol Rev* 12: 210–223.
- Marin-Neto JA, Cunha-Neto E, Maciel BC, Simoes MV (2007) Pathogenesis of chronic Chagas heart disease. *Circulation* 115: 1109–1123.
- Hontebeyrie M, Truyens C, Brenière SF (2010) Pathological consequences of host response to parasite in American Trypanosomiasis Chagas disease, One hundred years of re-research. edited by J Telleria and M Tibayrenc. Elsevier. pp 669–690.
- Brandariz S, Schijman A, Vigliano C, Arteman P, Viotti R, et al. (1995) Detection of parasite DNA in Chagas' heart disease. *Lancet* 346: 1370–1371.
- Aznar C, Lopez-Bergami P, Brandariz S, Mariette C, Liegeard P, et al. (1995) Prevalence of anti-R-13 antibodies in human Trypanosoma cruzi infection. *FEMS Immunol Med Microbiol* 12: 231–238.
- Levin MJ, Mesri E, Benarous R, Levitus G, Schijman A, et al. (1989) Identification of major Trypanosoma cruzi antigenic determinants in chronic Chagas' heart disease. *Am J Trop Med Hyg* 41: 530–538.
- Mesri EA, Levitus G, Hontebeyrie-Joskowicz M, Dighiero G, Van Regenmortel MH, et al. (1990) Major Trypanosoma cruzi antigenic determinant in Chagas' heart disease shares homology with the systemic lupus erythematosus ribosomal P protein epitope. *J Clin Microbiol* 28: 1219–1224.
- Levitus G, Hontebeyrie-Joskowicz M, Van Regenmortel MH, Levin MJ (1991) Humoral autoimmune response to ribosomal P proteins in chronic Chagas heart disease. *Clin Exp Immunol* 85: 413–417.
- Elies R, Ferrari I, Wallukat G, Lebesgue D, Chiale P, et al. (1996) Structural and functional analysis of the B cell epitopes recognized by anti-receptor autoantibodies in patients with Chagas' disease. *J Immunol* 157: 4203–4211.
- Kaplan D, Ferrari I, Bergami PL, Mahler E, Levitus G, et al. (1997) Antibodies to ribosomal P proteins of Trypanosoma cruzi in Chagas disease possess functional autoreactivity with heart tissue and differ from anti-P autoantibodies in lupus. *Proc Natl Acad Sci U S A* 94: 10301–10306.
- Ferrari I, Levin MJ, Wallukat G, Elies R, Lebesgue D, et al. (1995) Molecular mimicry between the immunodominant ribosomal protein P0 of Trypanosoma cruzi and a functional epitope on the human beta 1-adrenergic receptor. *J Exp Med* 182: 59–65.
- Mahler E, Sepulveda P, Jeannequin O, Liegeard P, Gounon P, et al. (2001) A monoclonal antibody against the immunodominant epitope of the ribosomal P2beta protein of Trypanosoma cruzi interacts with the human beta 1-adrenergic receptor. *Eur J Immunol* 31: 2210–2216.
- Mahler E, Hoebeke J, Levin MJ (2004) Structural and functional complexity of the humoral response against the Trypanosoma cruzi ribosomal P2 beta protein in patients with chronic Chagas' heart disease. *Clin Exp Immunol* 136: 527–534.
- Sepulveda P, Liegeard P, Wallukat G, Levin MJ, Hontebeyrie M (2000) Modulation of cardiocyte functional activity by antibodies against trypanosoma cruzi ribosomal P2 protein C terminus. *Infect Immun* 68: 5114–5119.
- Smulski C, Labovsky V, Levy G, Hontebeyrie M, Hoebeke J, et al. (2006) Structural basis of the cross-reaction between an antibody to the Trypanosoma cruzi ribosomal P2beta protein and the human beta1 adrenergic receptor. *FASEB J* 20: 1396–1406.
- Levy GV, Tasso LM, Longhi SA, Rivello HG, Kyto V, et al. (2011) Antibodies against the Trypanosoma cruzi ribosomal P proteins induce apoptosis in HL-1 cardiac cells. *Int J Parasitol* 41: 635–644.
- Warne T, Serrano-Vega MJ, Baker JG, Moukhametjanov R, Edwards PC, et al. (2008) Structure of a beta1-adrenergic G-protein-coupled receptor. *Nature* 454: 486–491.
- Muller S, Couppez M, Briand JP, Gordon J, Sautiere P, et al. (1985) Antigenic structure of histone H2B. *Biochim Biophys Acta* 827: 235–246.
- Otwinowski Z, Minor W, Charles W. Carter Jr. (1997) [20] Processing of X-ray diffraction data collected in oscillation mode. *Methods in Enzymology*: Academic Press. pp 307–326.
- Navaza J (1994) AMoRe: an automated package for molecular replacement. *Acta Crystallographica Section A* 50: 157–163.
- Emsley P, Cowtan K (2004) Coot: model-building tools for molecular graphics. *Acta Crystallogr D Biol Crystallogr* 60: 2126–2132.
- Lopez Bergami P, Scaglione J, Levin MJ (2001) Antibodies against the carboxyl-terminal end of the Trypanosoma cruzi ribosomal P proteins are pathogenic. *FASEB J* 15: 2602–2612.
- Stanfield RL, Zemla A, Wilson IA, Rupp B (2006) Antibody elbow angles are influenced by their light chain class. *J Mol Biol* 357: 1566–1574.

34. Mahler M, Kessenbrock K, Raats J, Williams R, Fritzler MJ, et al. (2003) Characterization of the human autoimmune response to the major C-terminal epitope of the ribosomal P proteins. *J Mol Med* 81: 194–204.
35. Tutor AS, Penela P, Mayor F, Jr. (2007) Anti-beta1-adrenergic receptor autoantibodies are potent stimulators of the ERK1/2 pathway in cardiac cells. *Cardiovasc Res* 76: 51–60.
36. Soares MR, Bisch PM, Campos de Carvalho AC, Valente AP, Almeida FC (2004) Correlation between conformation and antibody binding: NMR structure of cross-reactive peptides from *T. cruzi*, human and *L. braziliensis*. *FEBS Lett* 560: 134–140.
37. Warne T, Moukhametzianov R, Baker JG, Nehme R, Edwards PC, et al. (2011) The structural basis for agonist and partial agonist action on a beta(1)-adrenergic receptor. *Nature* 469: 241–244.
38. Peter JC, Wallukat G, Tugler J, Maurice D, Roegel JC, et al. (2004) Modulation of the M2 muscarinic acetylcholine receptor activity with monoclonal anti-M2 receptor antibody fragments. *J Biol Chem* 279: 55697–55706.
39. Peter JC, Eftekhari P, Billiald P, Wallukat G, Hoebeke J (2003) scFv single chain antibody variable fragment as inverse agonist of the beta2-adrenergic receptor. *J Biol Chem* 278: 36740–36747.
40. Mijares A, Lebesgue D, Wallukat G, Hoebeke J (2000) From agonist to antagonist: Fab fragments of an agonist-like monoclonal anti-beta(2)-adrenoceptor antibody behave as antagonists. *Mol Pharmacol* 58: 373–379.
41. Sterin-Borda L, Borda E (2000) Role of neurotransmitter autoantibodies in the pathogenesis of chagasic peripheral dysautonomia. *Ann N Y Acad Sci* 917: 273–280.
42. Labovsky V, Smulski CR, Gomez K, Levy G, Levin MJ (2007) Anti-beta1-adrenergic receptor autoantibodies in patients with chronic Chagas heart disease. *Clin Exp Immunol* 148: 440–449.
43. Wallukat G, Munoz Saravia SG, Haberland A, Bartel S, Araujo R, et al. (2010) Distinct patterns of autoantibodies against G-protein-coupled receptors in Chagas' cardiomyopathy and megacolon. Their potential impact for early risk assessment in asymptomatic Chagas' patients. *J Am Coll Cardiol* 55: 463–468.
44. Mao W, Fukuoka S, Iwai C, Liu J, Sharma VK, et al. (2007) Cardiomyocyte apoptosis in autoimmune cardiomyopathy: mediated via endoplasmic reticulum stress and exaggerated by norepinephrine. *Am J Physiol Heart Circ Physiol* 293: H1636–1645.
45. Jahns R, Schlipp A, Boivin V, Lohse MJ (2010) Targeting receptor antibodies in immune cardiomyopathy. *Semin Thromb Hemost* 36: 212–218.
46. Nussinovitch U, Shoenfeld Y (2010) The Clinical Significance of Anti-Beta-1 Adrenergic Receptor Autoantibodies in Cardiac Disease. *Clin Rev Allergy Immunol*.
47. Nussinovitch U, Shoenfeld Y (2011) The Diagnostic and Clinical Significance of Anti-Muscarinic Receptor Autoantibodies. *Clin Rev Allergy Immunol*.
48. Rosenbaum MB, Chiale PA, Schejman D, Levin M, Elizari MV (1994) Antibodies to beta-adrenergic receptors disclosing agonist-like properties in idiopathic dilated cardiomyopathy and Chagas' heart disease. *J Cardiovasc Electrophysiol* 5: 367–375.
49. Levin MJ, Kaplan D, Ferrari I, Arteman P, Vazquez M, et al. (1993) Humoral autoimmune response in Chagas' disease: Trypanosoma cruzi ribosomal antigens as immunizing agents. *FEMS Immunol Med Microbiol* 7: 205–210.
50. Lawrence MC, Colman PM (1993) Shape complementarity at protein/protein interfaces. *J Mol Biol* 234: 946–950.